This article has been accepted for publication in a future issue of this journal, but has not been fully edited. Content may change prior to final publication. Citation information: DOI 10.1109/ACCESS.2017.2694853, IEEE Access

Smart Metering Wireless Networks at 169 MHz

Marina Barbiroli, Franco Fuschini, Giovanni Tartarini, *Member, IEEE*, and Giovanni Emanuele Corazza, *Senior Member, IEEE*

***Abstract* — Intelligent metering systems are being rolled-out on a large-scale worldwide, enabling consumers to make informed choices about consumption patterns and energy saving, while supporting the development of new retail services and products. Unfortunately, the lack of established and shared international standards represents a serious hindrance to be overcome for a complete development of a profitable market. The identification of suitable communication protocols and cost-effective network architectures represent a challenging aspect.**

In this framework, different network design solutions for wireless smart metering systems at 169 MHz are considered and investigated in this paper, aiming at cost efficient deployment based on extensive re-use of existing infrastructures in urban scenarios, namely macro-cellular and lighting networks.

Coverage assessment and frequency planning issues are addressed, together with an "ad hoc" measurement campaign carried out to fill the gap in the knowledge of urban propagation in the 169 MHz band. Results show that cost-effective deployment of the intelligent metering network is achievable. Notably, a spatial reuse factor larger than the overall number of available frequency channels might be necessary, thus meaning that the spectral resources shall be also allocated according to a time division scheme where the hubs are switched off at turn. Anyway, this requirement should not affect the overall reading rate in practical applications.

***Index Terms*—Smart Metering, Network Planning, Wireless Propagation, 169 MHz band.**

I. Introduction

The dramatic and seemingly endless increase in the urbanization process currently on-going worldwide is raising problems and concerns about the perceived quality of life in large, chaotic and dense urban contexts. Smart and effective solutions must be conceived and deployed in order to tackle the manifold issues related to public and private transport, traffic, healthcare, supplying of goods and resources, as well as their management and distribution. These solutions commonly rely on strong technology support, basically made of sensors and devices spread throughout the urban layout, together with the corresponding management and control communication networks and the related applications and services for improved urban sustainability and efficiency [1],[2]. The urban conglomerate, enriched by such embedded technological infrastructures, is often referred to as a 'Smart City'.

In this framework, the pressing necessity for effective and careful use of energy, fuels and natural resources is leading to a tremendous growth in smart meters deployment, which can contribute to manage energy/gas/water distribution and consumption more efficiently than traditional utility meters. 'Smart metering system', or 'Advanced metering infrastructure', means an electronic system that can control energy, gas, or water consumption providing more information than a conventional monitoring system, by means of some form of electronic communication [3].

Both institutional initiatives and technical developments are being beneficial for the widespread distribution of smart metering systems. On the one hand, governments, public and industrial institutions are in fact promoting advanced metering applications [4]-[9], in order to increase the citizens' familiarity with the technology and their awareness about the related benefits. On the other hand, careful technical efforts are also requested for the reliable interconnection and management of such large amounts of devices; in particular, wired links are usually exploited for electrical meters, whereas wireless solutions are mainly employed for gas/water distribution monitoring [10], [11].

With particular reference to the wireless option, consolidated international standards for smart metering applications are yet to be defined. Unfortunately, the lack of established agreements on key aspects as the frequency bands, the communication protocol, the interference mitigation schemes and the network architecture, hinders the interoperability between different devices and therefore is delaying the massive diffusion of wireless metering services. Therefore, investigations aiming at identifying cost-effective network layouts in specific frequency bands are necessary contributions to the desired standardization process.

According to the hierarchical structure often referred to for a smart grid network, made of three different interconnected network layers, namely Home Area Network (HAN, including the intelligent electric appliances at the customers' level), Neighbourhood Area Network (NAN, related to the communication between the meters and a hub or data concentrator) and Wide Area Network (WAN, incorporating the nodes processing the data and therefore controlling the whole network), this work is focused on NAN. In particular, two different deployment strategies for a wireless smart metering network are analysed and compared. In both cases, the network aims at exploiting already available infrastructures that are nowadays rather common in every urban and suburban environment, namely the base stations

Manuscript received……….

The authors are with the Alma Mater Studiorum – University of Bologna, Dep. of Electrical, Electronic and Information Engineering "G. Marconi" (DEI), Viale Risorgimento 2, IT-40136 Bologna, Italy (e-mail: marina.barbiroli, franco.fuschini, giovanni.tartarini, giovanni.corazza @unibo.it).

(BSs) of macro-cellular networks, and the lampposts of public lighting networks. The analysis is in particular carried out in the 169 MHz frequency band, due to its better performance in terms of wireless propagation and hence building penetration [11]; extension to different frequency ranges is clearly possible.

In order to fully characterize the different network solutions, coverage assessments are carried out, i.e. related to the electromagnetic propagation conditions, and issues concerning the spatial and temporal re-use of the available frequency channels are addressed.

The paper is organized as follows: on-going activities on smart-metring evolution and development are summarized in Section II, whereas alternative architectures are presented in Section III. Sections IV and V deal with propagation issues for coverage assessment, including an “ad hoc” measurement campaign, and frequency planning evaluations, respectively. Conclusions are finally drawn in Section VI.

II. Smart Metering: Current Scenarios and Future Prospects

The availability of enhanced smart meter devices may potentially improve efficiency and reliability of metering networks, enable new services and empower consumers to make better informed decisions on individual energy, water or gas consumption. Therefore, advanced meters represents a key element for most of worldwide policies for sustainability and development and for competitive and valuable markets.

A. Worldwide survey of the on-going trends

In this framework, several trials and pilot projects spurring towards a widespread diffusion of advanced metering applications are being promoted by government investments and fiscal incentives, i.e. governments and public institutions frequently represent the principal drivers of growth in the global market for intelligent metering through mandated use and incentives.

At global level, several countries have enacted legislation mandating adoption of smart metering networks, as part of broader clean energy initiatives.

In the context of the 3rd Energy Package aiming at creating a single European gas and electricity market [4], [5], EU Member States have committed to roll out close to 200 million smart meters for electricity and 45 million for gas by 2020 at a total potential investment of € 45 billion. By 2020, it is expected that almost 72% of European consumers will have a smart meter for electricity while 40% will have one for gas.

In the U.S., as promoted by the Smart Grid Investment Grant program under the American Recovery and Reinvestment Act of 2009 [6], electric utilities in 2016 had about 70 million smart metering infrastructure installations and about 88% were residential customers, making up more than half of all households in the country.

According to [7], the installed base of smart meters in China will grow up to 377 million units by 2020, fostered by the 12th Five-year Plan on Energy Development [8], and the Strategic Action Plan on Energy Development (2014-2020) [9]. Furthermore, the Japanese TEPCO (Tokyo Electric Power Company) has announced plans to deploy 80 million smart meters over the next decade, while pilot projects are taking place in India to set the stage for extensive smart meter deployments that are expected to eventually total more than 150 million new devices.

B. Wireless and wired solutions for meters interconnection

Both wired and wireless communications can be exploited to detect and poll smart meters. In the former case, power line communications (PLC) probably represent the most common solution for the measurement of electricity usage, although xDSL and Passive Optical Network represent alternative options. Wireless technologies better fit water and gas distribution networks, where the smart meters can seldom rely on existing wired connections for communication [10],[11]. With reference to the on-going trials, wireless metering services and applications can be arranged in both licensed and unlicensed bands [10]. However, due to superior propagation characteristics [11], low-power requirements and less congestion in unlicensed band, the resort to sub-GHz bands currently seems widely preferred among the wireless options: 915 MHz in the US, 169 MHz, 433 MHz and 868 MHZ in the EU, 490 MHz in China and 920 MHz in Japan. In the European context, the 169 MHz band has been in particular relocated to specific metering applications [12], and pioneering activities are carried out in Italy, where a modernization of the gas distribution network is currently going on and at least 60% of residential premises will be equipped with 169 MHz advanced meters by the end of 2018 [13].

Compared to other frequency ranges, the 169 MHz band allows good performance in terms of coverage and building penetration/installation loss (meters often experience adverse propagation conditions, since they can be likely placed in the buildings' basement, inside metal cabinets etc.) and battery energy consumption, still ensuring a sufficient bitrate at the same time [11]. These favorable propagation properties are highlighted in Table I, where the free space excess loss is reported for different frequencies with respect to (wrt) 169 MHz, together with the related mean value of the Building Penetration Loss (<BPL>) [11].

The increasing propagation loss with frequency shown in the table straight impacts network performances, e.g. in terms of coverage extension and network layout, and this outcome would be even further stressed if propagation in real environment instead of ideal free space conditions were considered.

TABLE I
Comparison between different frequencies in terms of excess loss with respect to 169 MHz and <BPL>

Frequency [MHz]	**Available Technology/ Standard**	**Excess Loss wrt 169 MHz [dB]**	**<BPL> [dB]**
169	W-MBUS	0	7.5
500	--	9.5	11

This article has been accepted for publication in a future issue of this journal, but has not been fully edited. Content may change prior to final publication. Citation information: DOI 10.1109/ACCESS.2017.2694853, IEEE Access

800/900	LTE, RFID, GSM, GPRS, NB-IoT	14.5	12
2400	WiFi, ZigBee, 802.15.4g/e	23.0	15
3500	WiMAX	26.3	17

C. *Standardization issues*

With special reference to the wireless option, the lack of established international standards for both the communication protocol and the network architecture currently represents a serious hindrance to be still overcome for a complete development of a profitable market. Standards are of course important, because they ensure reliability, effective communication, interoperability of smart meter devices of different suppliers and promote healthy markets, lowering down both short and long-term costs. Different wireless standards as GSM/GPRS, Wireless M-Bus [14], IEEE 802.15.4g/e (Wireless Smart Utility Networks Alliance, Wi-SUN), Wi-Fi, ZigBee, WiGRID (a WiMAX technology based on IEEE 802.16e standard for utilities and industrial applications [15]) as well as LTE and Narrowband IoT (NB-IoT) [16] are so far under investigation across different countries and/or may represent valuable standardization options for smart metering communications.

In this framework, the European Commission and the European Free Trade Association mandated in 2009 CEN, CENELEC and ETSI (Mandate M/441) to develop an open architecture for utility meters involving communication protocols enabling interoperability (smart metering). This led to a Technical Report [17], which identifies the functional entities and communications interfaces for the forthcoming communications standards. Furthermore, the attention devoted to smart grid and advanced metering applications by public and private steering initiatives as the 5G Infrastructure Public Private Partnership (5GPPP) can also contribute to the development of shared agreements and technical standards for the smart metering market and technology [18].

In the U.S. the American National Standards Institute has published the Code for Electricity Metering [19] describing acceptable in-service performance levels for meters and devices used in revenue metering, and including information on recommended measurement standards, installation requirements, test methods, and test schedules. A communication protocol for smart houses (Echonet Lite), has been also approved by the Japanese Ministry of Economy, Trade and Industry and has then become an ISO/IEC international standard [20].

D. *Cost-benefit considerations*

Smart meter success of course depends on a positive cost-benefit balance. Efficient operation of the meter device and its associated network represents a crucial aspect to fully take advantage of an intelligent utility network.

Upgrading the distribution networks of goods like electricity, water or gas to a ‘smarter level’ is expected to produce manifold advantages and widespread benefits for all the involved players. Starting from the end users, smart metering can in general represent an enabler for a more effective and thriftier usage of resources [21]; e.g., consumers can receive real-time information about their consumption profile and the corresponding expenses, thus fostering cost reduction by increasing consumption during off-peak cheaper tariff periods. In the electricity network, the possibility of exploiting renewable-energy has led to the new paradigm of distributed generation, where smart meters play a key role. Furthermore, advanced metering overcomes the need for estimated readings, since billings can take into account what actually consumed during the billing period. Finally, a faster restoration from a service outage can be also pursued, since suppliers can more easily track unexpected breakdowns and leakages. Further profits for the utilities of course come from labor reduction, since the conventional practice of on premise meters reading becomes no longer necessary. Advanced metering can also produce benefits on a global scale [21], since it can represent a contribution in the fight on climate change, resulting in reduced waste and/or more efficient use of natural resources. Finally, smart metering may support governments to implement liberalization of markets related to the distribution of energy/water.

From a strict financial perspective, changing energy usage, automatic meter readings, and easier management of the energy network can produce large savings and guarantee the return of investment. According to the director of policy and communications at Smart Energy GB (Great Britain), the capital outlay in the national campaign for the smart meters rollout will be far outweighed by the savings - of more than £17 billion - that smart meters will generate throughout the energy system [22]. This expectation is further supported by the Italian electric power sector, where the return on investment took place 5 in years only.

E. *Network Architectures*

As already mentioned, the upgrade of the electricity network can be easily and naturally achieved through wired solutions (like PLC), thus fully re-using the existing infrastructure. In other cases (e.g. gas/water distribution), this is not as much possible, and the cost/effort estimate must take into account the deployment of the whole wireless network and not only the replacing of the meters. In this framework, system design should explore and identify the less expensive network architectures.

Wireless RF mesh networks can represent an effective solution [10], where thousands of connected devices (appliances, lampposts, vehicles, smartphones, etc.) may act as flexible, available and reliable nodes for routing data from the smart meters. This solution is clearly cost-effective, requiring a light, simple dedicated infrastructure, but at the same time it requires the IoT paradigm fully accomplished in order that it is also reliable, and this is something not already available so far.

In the meanwhile, the availability of wide spread infrastructures over the territory, such as mobile cellular networks [10] or lighting networks, can be exploited to speedup the deployment of multi-service intelligent metering systems. In fact, the possibility of (partly) re-using existing infrastructures may represent a key aspect to limit the overall cost of the wireless metering network, providing a large number of sites (the cellular base stations or the lampposts) which could potentially host the nodes of the advanced metering system. In this regard, Telefonica has recently proposed a smart meter network layout in the UK based on its existing cellular rollout.

Within this framework, the analysis carried out in the following sections investigates the main issues related to the design of a wireless smart metering network which exploits existing infrastructures commonly available in urban and suburban contexts.

III. Cost Effective Architectures for Smart metering wireless networks

Whilst awaiting flexible and light network architectures e.g. supported by IoT technologies and applications, a wireless metering system currently consists of an amount of meters spread over a certain area which wirelessly transmit data (e.g. related to the consumption of goods like water, gas, etc.) towards a hub (or data collector). Then, the hub routes the overall data traffic to the network nodes devoted to the management and processing of the information by means of wired or wireless point-to-point connections. It is worth noticing that consumption data transmissions from the meters likely occur upon specific inquiries raised by the hub, that means they can be properly scheduled in time. Moreover, the hubs might also occasionally send safety commands to handle possible emergencies (e.g. to trigger the closing of some safety valves to avoid dangerous leak of water or gas). Of course, both the interrogation and the command signals propagate from the data collector to the meter, i.e. two-way wireless links must be set-up. The hubs can be mobile, i.e. placed on top of traveling vehicles, or fixed, i.e. placed in proper, suitable locations within the service area.

In order to investigate the possibility of exploiting existing infrastructure, the following two main architectures are here envisaged and analysed (Figure 1.):

- *cellular based layout,* where the hubs are co-located with the BSs of a macro-cellular wireless network for mobile, personal communications; with reference to the hub antenna radiation properties, a 120º tri-sectorial case solution is considered to be typical [23]-[25];
- *lampposts based layout*, where the hubs equipped with an omnidirectional antenna are placed on the lampposts of a public lighting network.

The proposed architectures are analysed and compared hereafter assuming the meters located indoor and the wireless communications occurring in the 169 MHz band, which should allow more reliable propagation conditions of wireless signals as already referred to in the previous section.

Nevertheless, it is worth noticing that the proposed analysis can be extended to different frequency bands. Moreover, different frequency bands (e.g. 169 MHz and 868 MHz) can be used together in the same architecture to overcome interference issues in unlicensed bands, especially in a future view of multi-utilities/multi-services and smart city. As a matter of fact the considered solutions are independent of the type of sensor (meter), thus representing a multi-service approach which would guarantee economies of scale and shared investment costs and network management between different services and/or operators (gas, water, temperature, waste, etc.).

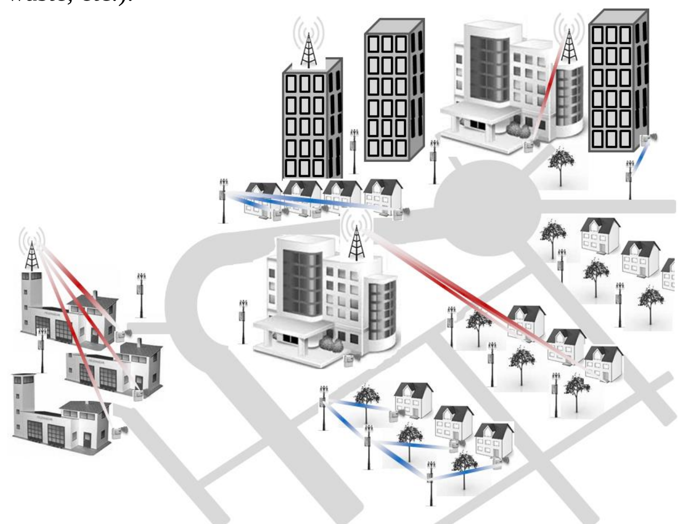

Figure 1. Wireless architecture with fixed hubs exploiting the existing mobile cellular network (red links) or the existing lighting network (blue links).

IV. Cell Extension in a Wireless Metering Network

In order to achieve an extensive infrastructure re-use, the required average dimension of the cell around each hub must comply with the common inter-site distance in a cellular network (cellular based layout) or with the usual spacing between lampposts (lampposts based layout).

In a wireless metering system, the cell extension can be limited by both the coverage related to the signal-to-noise distribution over the area and the maximum amount of smart meters that can be detected in the required reading period.

The coverage extent (R_1 in the following) is basically set by the power budget equation, where system and link parameters as the receiver sensitivity, the transmitted power, the antennas gain and polarization, together with the propagation losses are taken into account.

The cell extension restriction related to the requirement on the detection time depends of course on the maximum duration of the reading period, but also on the average time for data acquisition from a single meter and the meters' spatial density. The corresponding cell radius is referred to as R_2 in the following.

Finally, the actual cell extension is given by the minimum between R_1 and R_2.

A. Coverage assessment: evaluation of R_1

A general, simple but effective method to assess the radio coverage, taking also into account the fading effects suffered by the wireless signals, is based on the 'link budget' equation

This article has been accepted for publication in a future issue of this journal, but has not been fully edited. Content may change prior to final publication. Citation information: DOI 10.1109/ACCESS.2017.2694853, IEEE Access

[23], that for a smart-metering wireless link can be written as [11]:

$$P_{RX\_SENS} = P_{TX} + G_{TX} + G_{RX} - \langle \mathrm{PL}(R_1) \rangle - \langle \mathrm{BPL} \rangle - \langle \mathrm{IL} \rangle - \mathrm{M_f} \quad (1)$$

where:

- P_{TX} is the radiated power. The meter-to-hub communication is here assumed as the critical link, since transmissions from the meter will especially undergo some power-restriction in order to save the on-board battery life;
- P_{RX_SENS} is the receiver sensitivity;
- $G_{TX/RX}$ is the transmitter/receiver antenna gain. As the meter antenna dimension is quite smaller than the wavelength, a negative value of the gain, due to a poor radiation efficiency, should be expected, whereas for a weakly positive value can be likely assumed for the hub;
- <PL(R)> is the outdoor, median path loss experienced at the cell boundary;
- <BPL> is the average Building Penetration Loss (BPL) [11];
- <IL> is the mean installation loss, as defined in [11];
- M_f is a proper fading margin that takes into account large-scale signal fluctuations due to both shadowing and outdoor-to-indoor propagation effects [11]. The M_f value can be quickly computed based on the cell coverage probability P_C (that is a project target requirement) and on the value of the standard deviation σ_0 of the normal distributions describing the overall signal fluctuations. As argued in [11], σ_0 (in dB-unit) can be expressed as:

$$\sigma_{0,\mathrm{dB}} = \sqrt{\sigma_{\mathrm{SH}}^2 + \sigma_{\mathrm{BPL}}^2} \quad (2)$$

where σ_{SH} and σ_{BPL} respectively account for the outdoor shadowing and the deviations from the mean BPL.

Although the parameters appearing in eq. (1) may of course change case by case, they have been here fixed to the reference values listed in Table II.

TABLE II
Reference values for the parameters in eq. (1)

PARAMETER	REFERENCE VALUE
P_{TX}	20 dBm
P_{RX_SENS}	-110 dBm
G_{TX}	-5 dB
G_{RX}	2 ÷ 5 dB
<PL(R)>	Details in sub-sections IV.A1 and IV.A2
<BPL>	7.5 dB [11]
<IL>	0 dB (INDOOR) [11] 7 dB (INDOOR, METER IN A CLOSE HOUSING) [11] 13 dB (BASEMENT) [11]
σ_{SH}	5.5 dB [26]/ 9.1 dB (section IV.A2)
σ_{BPL}	4.5 dB [11]

A1. Cellular wireless network layout

If a mobile, macro-cellular network deployment is considered as network layout for the smart metering system, propagation models such as the Standard Propagation Model (extension of the Hata model [27] nowadays used in radio network planning tools like ATOLL® [28]) are available in literature for the analytical formulation of <PL(R)>. Based on such analytical expressions, the coverage radius R_1 has been computed from eq. (1) in some reference cases, as listed in Table III.

TABLE III
Coverage radius R_1 for the mobile, cellular network layout.

		P_C = 90%	P_C = 95%
METER LOCATION	INDOOR	2040 m	1700 m
	INDOOR IN A CLOSE HOUSING	1290 m	1070 m
	BASEMENT	870 m	720 m

Overall, the cell radius values in Table III seem compliant with the usual, inter-site distance in a mobile, macro-cellular network, thus supporting the general idea of a cost-effective deployment of the smart metering network exploiting already existing cellular infrastructures.

As a first term of comparison, the coverage radius has been also computed at the frequency of 900 MHz (Indoor case, P_C = 90%), of course properly updating – if needed - the parameters to be included in the link budget equation (Table II). The value of R_1 has turned out to be equal to 980 m, i.e. nearly the half of what achieved at 169 MHz, corresponding to a cell coverage area reduced by approximately a factor 4.

A2. Lighting network layout

Due to the lack of available statistical propagation models at 169 MHz when both the Tx and the Rx are located below the average level of the surrounding buildings, an “ad hoc” measurement campaign has been carried out in the city of Bologna (Italy) in dense urban and suburban environment, aiming at modelling the average dependence of path loss on link distance, together with the standard deviation of the received signal fluctuations due to shadowing effects (σ_{SH} in eq. (2)).

The measurement set up consisted of an HP 8663A synthesized signal generator to produce the 169 MHz CW signal, that was then boosted by means of a Mini-Circuits TIA 1000-4 amplifier and finally radiated through a two-element Yagi antenna (LeA R-Y 212 NH) having a size nearly equal to 61.5 cm × 95.5 cm; 50 ohm coaxial cables have been used to connect the different blocks. The receiver, a Telit Demo Case with two RF modules (ME50-169 and ME70-169) [29], was equipped with an helical monopole antenna (EAD H169-SMA) with a length of approximately 14 cm and equipped with a circular ground plane, and finally set on a mobile support (Figure 2.) in order to easily displace the receiver in different positions along city roads.

This article has been accepted for publication in a future issue of this journal, but has not been fully edited. Content may change prior to final publication. Citation information: DOI 10.1109/ACCESS.2017.2694853, IEEE Access

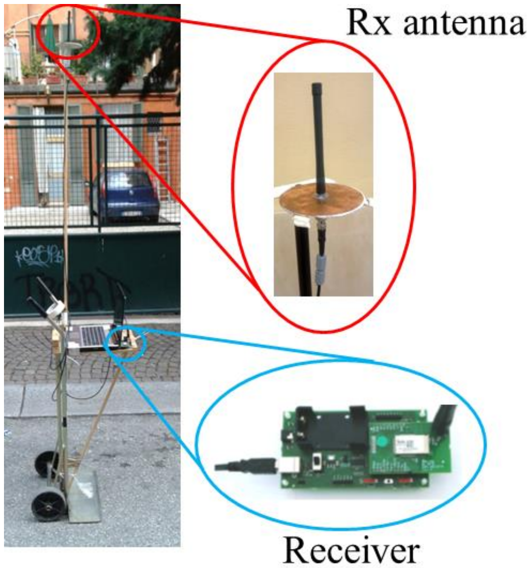

Figure 2. The receiver utilized in the measurement campaign carried out in Bologna, mounted on a mobile support.

In the suburban scenario, the transmitter was located at 5.5 m height and the Received Signal Strength (RSS) values have been collected over 100 receiving points (Figure 3. **)**. In the urban environment, the Tx height was raised to 8 and 12 m (i.e. representative of the height of lampposts) and the Rx was moved at street level over 335 locations.

Figure 3. Measurement routes deployed in the suburban scenario.

The RSS samples have been then spatially averaged over a sliding window containing at least 3 different Rx locations, in order to remove (or at least reduce) possible fast fading effects.

Finally, the least square errors method was applied to the averaged data in order to get the best K and α values corresponding to the optimal representation of the average range dependence of path-loss through a straight line (in a log-log scale) as follows:

$$\langle PL(R) \rangle = K + 10\alpha \log_{10} R \qquad (3)$$

The path-loss factor α in eq. (3) of course describes the slope of the fitting straight line, and fundamentally takes into account the 'average amount of obstruction' suffered by the wireless signals as they propagate through the outdoor radio channel; instead, K is the intercept coefficient accounting for major link parameters as the wavelength and the height of the antennas. R is of course the link distance.

The deviations of the measured RSS values from the regression curve (3) have been also computed, in order to achieve an experimental characterization of the shadowing fluctuations. The corresponding cumulative distribution functions for the considered scenarios are shown in Figure 4. , together with a normal approximation for the same std. dev σ_{SH}. Owing to the rather satisfactory agreement, a complete statistical characterization of the large-scale, narrowband propagation effects can be then based on the α and σ_{SH} values.

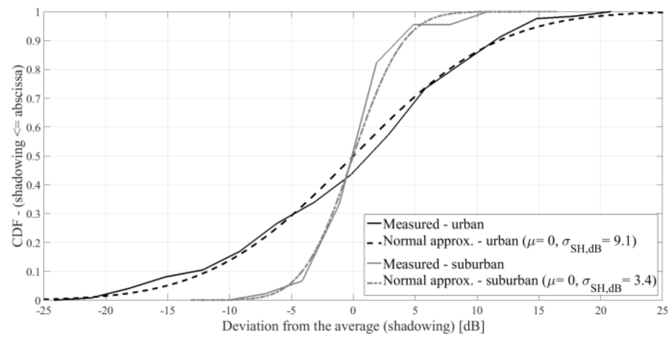

Figure 4. Large scale fading experimental distribution and Gaussian fitting.

The achieved values of α, σ_{SH} and K are summarized in Table IV for the investigated scenarios.

TABLE IV

Path Loss exponent α and shadowing fluctuations σ_{SH} values for suburban and urban environment.

	α	σ_{SH} [dB]	K [dB/m]
SUBURBAN	4.3	3.5	-20.5
URBAN	5.3	9.1	-12.9

Based on the experimental characterization of radio propagation for the lampposts based layout, the corresponding coverage radius R_1 have been then computed (see Table V) from the power budget (eq. 1) for the same coverage probability and reference indoor placement considered for the cellular layout.

TABLE V

Coverage radius R_1 for the urban lighting network layout.

		P_C = 90%	P_C = 95%
METER LOCATION	INDOOR	310 m	250 m
	INDOOR IN A CLOSE HOUSING	230 m	190 m
	BASEMENT	175 m	145 m

Results in Table V are likely larger than the usual distance

This article has been accepted for publication in a future issue of this journal, but has not been fully edited. Content may change prior to final publication. Citation information: DOI 10.1109/ACCESS.2017.2694853, IEEE Access

between lamppost in a (sub)urban lighting network, that therefore can also represent an already available infrastructure to host the data collectors of a smart metering wireless network.

B. *Maximum amount of manageable meters: evaluation of R_2*

The total number of meters (M_{tot}) included within a cell of the smart metering network can be expressed as:

$$M_{tot} = A_C \times \rho_m \tag{4}$$

being A_C the cell area and ρ_m the meters spatial density. Assuming each household basically owns a meter, then ρ_m can be estimated as:

$$\rho_m = \frac{\rho_i}{n_h} \tag{5}$$

where ρ_i represents the inhabitants spatial density (n. of inhabitants/km^2) and n_h is the average household size, e.g. equal to about 2.4 in the European area [30] and to approximately 2.5 for the USA [31].

If τ is the average time required to detect a single meter, and N_{ch} is the number of frequency available channels for each cell, then the overall detection time Δ for the whole amount of M_{tot} meters is equal to:

$$\Delta = M_{tot} \cdot \frac{\tau}{N_{ch}} = A_C \cdot \frac{\rho_i}{n_h} \cdot \frac{\tau}{N_{ch}} \tag{6}$$

In case a maximum allowed detection time (Δ_{max}) is set by the service requirements, eq. (6) immediately leads to a further constraint on the maximum cell extension ($A_{C,max}$). The corresponding radius R_2 can be therefore computed as:

$$A_{C,max} = \frac{\pi \cdot R_2^2}{n_s} = N_{ch} \cdot \frac{\Delta_{max}}{\tau} \cdot \frac{n_h}{\rho_i} \tag{7}$$

being n_s = 3 and n_s = 1 for the tri-sectorial and the omnidirectional case, respectively. The corresponding radius R_2 can be therefore computed as:

$$R_2 = \sqrt{\frac{n_s}{\pi} \cdot N_{ch} \cdot \frac{\Delta_{max}}{\tau} \cdot \frac{n_h}{\rho_i}} \tag{8}$$

Tables VI and VII respectively report the cell radius R_2 for an omnidirectional and a tri-sectorial case, and for some reference values of Δ_{max} and N_{ch}. It is worth noticing that $N_{ch} < 1$ is also considered in the tables, thus meaning that the cell is assigned with a single frequency channel not for the whole time, but rather part-time (e.g. N_{ch} = 0.5 corresponds to a resource availability for the 50% of time). This represents a clear difference between a smart metering network, where the reading of meters can be scheduled in time, and a wireless network for personal communications, where the radio resources should be basically available upon users' request at any time.

TABLE VI

Maximum reading distance R_2 of the smart metering cell assuming the hub equipped with an omnidirectional antenna (n_s = 1 in eq. (8)).

ρ_i = 7000 inh/km^2 (high-density populated area), τ = 100 msec, n_h = 2.4 [30]			
	Δ_{max} = 1 h	Δ_{max} = 1 day	Δ_{max} = 1 week
N_{ch} = 0.5	1.4 km	6.9 km	18.2 km
N_{ch} = 1	2.0 km	9.7 km	25.7 km
N_{ch} = 1.5	2.4 km	11.9 km	31.5 km

TABLE VII

Maximum reading distance R_2 of the smart metering cell assuming the hub equipped with three directive antennas (n_s = 3 in eq. (8)).

ρ_i = 7000 inh/km^2 (high-density populated area), τ = 100 msec, n_h = 2.4 [30]			
	Δ_{max} = 1 h	Δ_{max} = 1 day	Δ_{max} = 1 week
N_{ch} = 0.5	2.4 km	11.9 km	31.5 km
N_{ch} = 1	3.4 km	16.8 km	44.5 km
N_{ch} = 1.5	4.1 km	20.6 km	54.5 km

According to the cell radius values shown in Tables III and V (R_1) and in Tables VI-VII (R_2), radio coverage seems by far the most stringent constraint to the cell extension, being the amount of meters to be managed by each hub not the limiting factor.

V. Smart Metering Wireless Network Planning: Space-Time Reuse of Resources

According to [12], the number of available channels in the 169 MHz band is quite small (6/8); moreover, in order to limit possible co-channel interference a frequency spatial reuse greater than 1 will be likely necessary in every smart metering wireless network. Therefore, the number of frequency channels assigned to each hub can be supposed to be rather limited.

In contrast, the traffic from each meter can be expected to be quite small (few kilobytes at most [32]) and can be also scheduled in time, since inquiries from the hub should have a sporadic occurrence in most cases. Therefore, a time division access scheme can be also implemented, assigning the frequency channels to the hubs only for a certain amount of hours/day.

In case the hubs are supplied with omnidirectional antennas (as here assumed for the lampposts network layout), then the signal-to-interference ratio can be related to the cluster size m (or spatial reuse factor, i.e. the number of cells or sectors sharing all available resources) as (further explanations are included in the final Appendix) [24]:

$$\frac{C}{I} = \frac{1}{6} \cdot (3m)^{\alpha/2} \tag{9}$$

Conversely, if the hub sites are equipped with three directional antennas (as considered for the macro-cellular layout) the number of interferers reduces accordingly and eq. (9) can be reformulated as follows (details are again provided in the Appendix):

$$\frac{C}{I} = \frac{1}{2} \cdot (m)^{\alpha/2} \tag{10}$$

The path loss exponent (α) can be assumed equal to 3.5 for

This article has been accepted for publication in a future issue of this journal, but has not been fully edited. Content may change prior to final publication. Citation information: DOI 10.1109/ACCESS.2017.2694853, IEEE Access

the cellular layout with BSs 30 m high [27][28], and has been computed equal to 5.3 for the urban environment in the lighting network scenario (see Table IV).

It's worth noticing that the simple analytical procedure leading to eqs. (9) and (10) takes into account only the average dependence of both the useful (C) and the interfering (I) received power on the link distance, i.e. possible deviation from the mean power values due to shadowing effects are completely neglected. Therefore, the simple, closed-form expressions in eqs. (9)-(10) provide somehow an evaluation for the *average* signal-to-interference ratio experienced by a meter placed at the boundary of the cell it belongs to, when interfered by the nearest interfering meters placed in the centres of the corresponding cells. Therefore, the evaluation of the cluster size by setting the first term of eqs. (9)-(10) equal to the signal-to-interference "threshold value" $(C/I)_{th}$ would correspond to a a (C/I) distribution equal to $(C/I)_{th}$ only *on the average*. This is often considered not completely satisfactory, and therefore a better, safer m value is often achieved fixing the first term of eqs. (9) and (10) equal to $(C/I)_{th}$ increased by a proper *interference margin* M_I. The value of M_I can be computed from the statistical distribution of the signal-to-interference ratio as shortly discussed herein.

The interfering power I is of course the result of the different interfering contributions coming from the meters exploiting the same resources at the same time. Assuming such contributions exhibit spatial fluctuations compliant with statistically independent log-normal distribution, the overall interference can be still regarded as a log-normal random variable [33], [34]. Since the interfering meters belonging to the first tier are supposed at the same distance (D) from the interfered hub, the same mean value can be approximately assumed for the interfering signals. Furthermore, the same std. dev. $\sigma_{0,dB}$ can be also considered, as all the signals propagate under the same general conditions within the same environment. According to [33], the standard deviation of the whole interference can be expressed as:

$$\sigma_I\,[dB] = \frac{1}{0.23}\cdot\sqrt{\log_e\left\{1+\frac{K}{n_i}\cdot\left[e^{\left(0.23\cdot\sigma_{0,dB}\right)^2}-1\right]\right\}} \quad (9)$$

where K = 0.5 for the urban environment [35]. Based on eq. (2), the values here considered for $\sigma_{0,dB}$ are equal to 7.1 dB and to 10.15 dB for the macro-cellular and the lampposts network layout, respectively. In so far C_{dBm} and I_{dBm} are independent variables, then $(C/I)_{dB}=C_{dBm}-I_{dBm}$ is also a Gaussian variable with variance $\sigma^2_{C/I}=\sigma^2_C+\sigma^2_I$. The value of σ_I is of course provided by (9), whereas $\sigma_C = \sigma_{0,dB}$ has been considered. Table VIII reports $\sigma_{C/I}$ values for the two different architectures.

TABLE VIII
Standard deviation of the signal-to-interference ratio for the two architectures considered in this work.

	$\sigma_{C/I}$ URBAN
Omnidirectional coverage layout (lamppost)	12.4 dB
Tri-sector coverage layout (cellular)	8.8 dB

Based on the statistical parameters of the signal-to-interference ratio, the fading margin can be finally related to the probability $q_{C/I}$ that $(C/I)_{dB}$ exceeds the required threshold, i.e:

$$\Pr ob\left\{\left(\frac{C}{I}\right)_{dB} \ge \left(\frac{C}{I}\right)_{th,dB}\right\} = q_{C/I}$$

$$\frac{1}{2}\left[1+\mathrm{erf}\,\frac{\overbrace{\left(C/I\right)_{mean,dB}-\left(C/I\right)_{th,dB}}^{M_{I,dB}}}{\sigma_{C/I}\cdot\sqrt{2}}\right] = q_{C/I} \quad (10)$$

$$\frac{1}{2}\left[1+\mathrm{erf}\,\frac{M_{I,dB}}{\sigma_{C/I}\cdot\sqrt{2}}\right] = q_{C/I}$$

After the computation of the interference margin by means of eq. (10), the minimum cluster size for an effective network design can be quickly achieved setting the first term of eq. (9) – omnidirectional case – or eq. (10) – tri-sectorial case – equal to $(C/I)_{th,dB}+M_{I,dB}$. The corresponding results are summarized in Tables IX-X.

The cluster size values in Tables IX-X show that the better management of interference allowed by the resort to sectorization of course corresponds to a lower number of sites sharing the available frequency channels, and therefore to a shorter reuse distance.

TABLE IX
Cluster size predicted values assuming the hub equipped with an omnidirectional antenna

	$(C/I)_{th}$ = 6 dB	$(C/I)_{th}$ = 9 dB
Prob{C/I > C/I_{th}} = $q_{C/I}$ = 85 %	4	7
Prob{C/I > C/I_{th}} = $q_{C/I}$ = 95 %	7	9

TABLE X
Cluster size predicted values assuming the hub equipped with three directive antennas

	$(C/I)_{th}$ = 6 dB	$(C/I)_{th}$ = 9 dB
Prob{C/I > C/I_{th}} = $q_{C/I}$ = 85 %	3×3	3×4
Prob{C/I > C/I_{th}} = $q_{C/I}$ = 95 %	3×4	3×7

Furthermore, it can be noticed that a cluster size smaller than 7 is hardly achieved; as the available channels are 6 (or 8 at most), N_{ch} < 1 can be expected (as already considered in Table VI-VII). Therefore, the spectral resources should be likely allocated not only in space (between different cells or sectors of the cluster) but also in a time division scheme where the hubs might be switched off in turn and the detections of meters should be properly scheduled and carried out within the working periods only.

As long as the cell size is bounded by the coverage constraints (section III), eq. (6) can be then exploited to estimate the time Δ required for each hub to interrogate all the

This article has been accepted for publication in a future issue of this journal, but has not been fully edited. Content may change prior to final publication. Citation information: DOI 10.1109/ACCESS.2017.2694853, IEEE Access

meters located within the cell. The reading time is for instance evaluated in Table XI assuming the cell radius corresponding to the indoor case in Tables III and V, the cluster size compliant with $q_{C/I}$ = 85% and $(C/I)_{th,dB}$=9 dB. The values of the other parameters included in eq. (6) are reported in the table caption.

TABLE XI

Reading time assessment (τ=100 msec, n_h=2.4, overall number of available frequency channels = 6)

	Δ
Lighting network layout (R_1=310 m, m=7)	1 min. 43 sec.
Macro-cellular network layout (R_1=2040 m, m=12)	43 min.

According to the estimate of Δ in Table XI, many detections per day should be possible even with the restriction for the hubs to stay idle part of the time (N_{ch} < 1); that seems by far more than what should be actually necessary for many practical applications.

VI. Conclusions

In this paper, cost-effective network design strategies for smart metering wireless cellular systems at 169 MHz have been discussed and analysed. Although different wireless metering networks owned by different operators might simultaneously operate on the same area over this unlicensed band, sharing the same meters and arousing possible mutual interference, the planning issues related to the presence of multiple competing operators has not been addressed at this stage of the proposed study for the sake of simplicity.

The possibility of deploying the smart metering network re-using existing infrastructures commonly available in urban scenarios has been investigated with special reference to two different solutions, namely a macro-cellular and a lighting network layout

In both cases, issues related to the radio-coverage and the spatial and temporal sharing of the available spectral resources among the different cells have been addressed.

The cells' extension has turned out to be limited by propagation impairments, with coverage radius approximately ranging from 700 m to 2 km for the macro-cellular arrangement, and from 200 to 300 m for the lighting network solution. Such values are in general compliant with the distance between base stations and lampposts, respectively, thus supporting the idea of a cost-effective exploitation of already existing infrastructures.

With reference to the radio resource management, a spatial re-use factor larger than the overall number of available frequency channels has been achieved, thus meaning that the available channels should be necessarily shared in time according to a time division scheme, where the hubs are switched off in turn. Anyway, such constraint doesn't seem to represent a strong limitation, since the overall working period should be long enough to allow multiple detections of the meters per day, that can be supposed satisfactory for many practical applications.

Appendix

As a matter of fact, planning strategies for wireless cellular networks are usually discussed and investigated dividing the service area into non-overlapping cells with equal area and hexagonal shape [24], [25]. Although radio propagation in real environment is in general anisotropic and real cells are by far less regular, a uniform tessellation is fundamentally required to understand and model system concepts by means of effective but simple to use analytical formulations. Anyway, the cell radius is still defined for an hexagonal, cellular layout as the radius of the circle circumscribing each hexagonal cell, as also sketched in Fig. A1.

In this framework, the carrier to interference ratio is usually expressed as [24]:

$$\frac{C}{I} = \frac{1}{n_i} \cdot \left(\frac{D}{R}\right)^{\alpha} \tag{A1}$$

being n_i the number of interferers, α the path-loss factor, D the reuse-distance (i.e. the distance between cells assigned with the same radio resources) and R the cell radius. In particular, eq. (A1) holds for the up-link communications (meters-to-hub, referring to a smart metring wireless network), and takes into account only the interferers belonging to the "first tier", placed in the centre of the corresponding cells [24]. The same transmitted power is also supposed for each meter.

Assuming the hubs positioned in the centre of the cells (hexagons of side R in Fig. A1) and equipped with omnidirectional radiators in the horizontal plane, n_i = 6 (Fig. A1) and the cluster size can be related to the reuse distance to cell radius ratio as explained herein. First, the cluster size m can be expressed as the ratio between the cluster and the cell area:

$$m = \frac{A_{cluster}}{A_{cell}} \tag{A2}$$

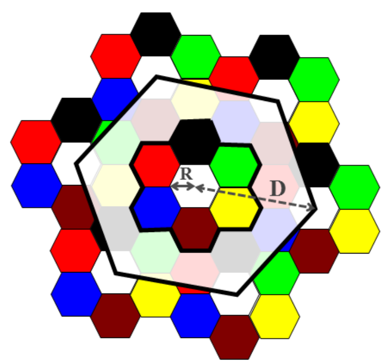

Figure A1 – Hexagonal tessellation, omnidirectional case. The different colors account for the different radio resources assigned to the cells.

The extension of the cluster can then be computed as one third of the area of the regular hexagon of side D having its vertexes in the centers of six nearest co-channel interfering cells [24]:

This article has been accepted for publication in a future issue of this journal, but has not been fully edited. Content may change prior to final publication. Citation information: DOI 10.1109/ACCESS.2017.2694853, IEEE Access

$$A_{cluster} = \frac{1}{3}\frac{6 \cdot D \cdot \left(\frac{D}{2}\sqrt{3}\right)}{2} = \frac{\sqrt{3}}{2} \cdot D^2 \qquad (A3)$$

Since A_{cell} is of course the area of an hexagon of side R, the following relation between m and (D/R) can be therefore achieved:

$$m = \frac{\frac{\sqrt{3}}{2} \cdot D^2}{\frac{3}{2} \cdot \sqrt{3} \cdot R^2} = \frac{D^2}{3R^2} = \frac{1}{3}\left(\frac{D}{R}\right)^2 \qquad (A4)$$

Based on eq. (A4), eq. (9) can be now immediately achieved from eq. (A1).

A widely exploited solution to reduce interference is sectorization [24], [26]: the radio resources available at each cell are split into N groups, and each group is then devoted to the management of the wireless communications occurring over 1/N of the cell by means of N directive antennas properly arranged at the BS site. N is commonly equal to 3, corresponding to an angular width of the directive antennas radiation lobe nearly equal to 120º. This situation is sketched in Figure. A2. Although the number of nearest sectors assigned with the same radio resources is still 6, harmful interfering signals can actually come from 2 of them only (as also highlighted in Figure. A2), due to the directive radiation patterns of the BSs antennas.

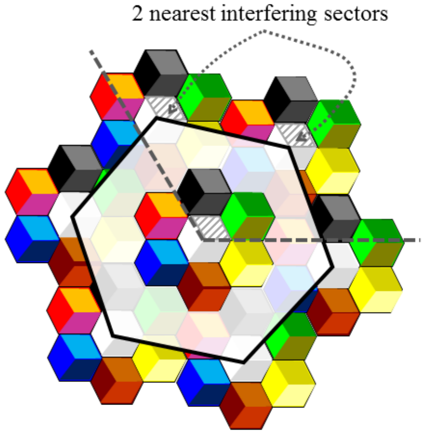

Figure A2 – Hexagonal tessellation with sectorization. The different colors account for the different radio resources assigned to the sectors.

With reference to the cluster size, the same geometrical considerations which lead to eq. (A2) still hold also for the sectorial arrangement. Conversely, since a sector corresponds to one third of a hexagon of side R, its area can be expressed as:

$$A_{sector} = \frac{1}{3}\frac{6 \cdot R \cdot \left(\frac{R}{2}\sqrt{3}\right)}{2} = \frac{\sqrt{3}}{2} \cdot R^2 \qquad (A5)$$

The corresponding cluster size is therefore equal to:

$$m = \frac{\frac{\sqrt{3}}{2} \cdot D^2}{\frac{\sqrt{3}}{2} \cdot R^2} = \frac{D^2}{R^2} = \left(\frac{D}{R}\right)^2 \qquad (A6)$$

The substitution of eq. (A6) into the general expression (A1) clearly leads to the eq. (10) referred to in section V.

REFERENCES

[1] IEC, "Orchestrating infrastructure for sustainable Smart Cities", White Paper, http://www.iec.ch/whitepaper/pdf/iecWP-smartcities-LR-en.pdf, 2015;

[2] W. Ejaz, M. Naeem, A. Shahid, A. Anpalagan, M- Jo, "Efficient Energy Management for the Internet of Thongs in Smart Cities", IEEE Comm. Magazine, vol. 55, No. 1, pp. 84-91, January 2017;

[3] Definition from Article 2, point 28 of the Energy Efficiency Directive (2012/27/EU), OJ L315, 14.11.2012, p.1;

[4] DIRECTIVE 2009/72/EC of The European Parliament and of The Council of 13 July 2009, concerning common rules for the internal market in electricity and repealing Directive 2003/54/EC;

[5] DIRECTIVE 2009/73/EC of The European Parliament and of The Council of 13 July 2009, concerning common rules for the internal market in natural gas and repealing Directive 2003/55/EC;

[6] The American Recovery and Reinvestment Act of 2009 (Recovery Act) provided the U.S. Department of Energy with $4.5 billion to modernize the electric power grid and to implement Title XIII of the Energy Independence and Security Act (EISA) of 2007. https://www.smartgrid.gov/recovery_act/index.html;

[7] "Smart Meters. Smart Electric Meters, Advanced Metering Infrastructure, and Meter Communications: Global Market Analysis and Forecasts". https://www.navigantresearch.com/research/smart-meters;

[8] Notice of theState Council on Issuing the 12th Five-year Plan on Energy Development] (promulgated by the State Council, Jan. 1, 2013), available at http://www.gov.cn/zwgk/2013-01/23/content_2318554.htm.

[9] Notice of the General Office of the State Council on Issuing the Strategic Action Plan on Energy Development (2014-2020)] (promulgated by the General Office of the State Council, Guobanfa [2014] 31 Hao, June 7, 2014), available at http://www.gov.cn/zhengce/content/2014-11/19/content_9222.htm.

[10] Noelia Uribe-Pérez,, Luis Hernández, David de la Vega and Itziar Angulo "State of the Art and Trends Review of Smart Metering in Electricity Grids", Applied Science 2016, 6, 68; doi:10.3390/app6030068

[11] Fuschini, F.; Barbiroli, M.; Corazza, G.E.; Degli-Esposti, V.; Falciasecca, G., "Analysis of Outdoor-to-Indoor Propagation at 169 MHz for Smart Metering Applications," Antennas and Propagation, IEEE Transactions on Antennas and Propagation, vol.63, no.4, pp.1811,1821, April 2015, doi: 10.1109/TAP.2015.2399507;

[12] CEPT, ECC, ERC Recommendation 70-03 "Relating to the use of Short Range Devices (SRD)", Subsequent amendments, 27 May 2016;

[13] Regulatory Order ARG/gas 155/08, "Direttive per la messa in servizio dei gruppi di misura del gas, caratterizzati da requisiti funzionali minimi e con funzioni di telelettura e telegestione, per i punti di riconsegna delle reti di distribuzione del gas naturale", October 2008;

[14] BS EN 13757-4:2013, "Communication systems for meters and remote reading of meters . Wireless meter readout (Radio meter reading for operation in SRD bands)";

[15] http://wimaxforum.org/Page/Initiatives/WiGRID

[16] Y.-P. E. Wang, X. Lin, A. Adhikary, A. Grövlen, Y. Sui, Y. Blankenship, J. Bergman, and H. S. Razaghi, "A Primer on 3GPP Narrowband Internet of Things (NB-IoT)," submitted to IEEE Communications Magazine, June 2016;

[17] CEN/CLC/ETSI/TR 50572 Technical Report "Functional reference architecture for communications in smart metering systems", December 2011;

[18] 5G-Infrastructure-Association, "5G and Energy", September 2015 (available on-line at https://5g-ppp.eu/white-papers/)

[19] ANSI C12.1-2014, American National Standard for Electric Meters - Code for Electricity Metering standard by American National Standards Institute, 02/01/2016.
[20] https://echonet.jp/english/
[21] B. Neenan, R.C. Hemphill, "Societal Benefits of Smart Metering Investments", The Electricity Journal, vol. 21, No. 8, pp. 32-45, October 2008;

[22] http://www.telegraph.co.uk/finance/personalfinance/energy-bills/11975065/Smart-meters-will-cost-11bn-but-youll-be-lucky-if-yours-saves-you-30.html
[23] J. D. Parson "The Mobile Radio Propagation Channel", 2nd Edition Wiley, 2000;
[24] A. Goldsmith, "Wireless Communications", Cambridge University Press, 2005;
[25] H.L. Bertoni, "Radio Propagation for Modern Wireless Systems", Prentice Hall 2000;
[26] S.R. Saunders, A.A. Zavala, "Antennas and Propagation for Wireless Communication Systems", Wiley & Sons 2007];
[27] M. Hata, "Empirical formula for propagation loss in land mobile radio service", IEEE Trans. On Vehicular Technology, vol. VT-29, pp. 317-325, 1980;
[28] F Planning & Optimisation Software. ATOLL®. User Manual. version 3.3. FORSK, 2015. http://www.forsk.com/atoll/;
[29] 'ME50/70-169 Demo Case User Guide'. (http://www.telit.com/module/infopool/download.php?id=5318);
[30] Eurostat, statistics explained "People in the EU – statistics on household and family structures", available on line: http://ec.europa.eu/eurostat/statistics-explained/index.php/People_in_the_EU_%E2%80%93_statistics_on_household_and_family_structures;
[31] https://www.census.gov/hhes/families/files/graphics/HH-6.pdf;
[32] W. Luan, D. Sharp and S. LaRoy, "Data traffic analysis of utility smart metering network," 2013 IEEE Power & Energy Society General Meeting, Vancouver, BC, 2013, pp. 1-4. doi: 10.1109/PESMG.2013.6672750;
[33] L. F. Fenton, "The Sum of Log-Normal Probability distributions in scatter transmission system", IEEE Transactions on Communications, vol. 8, pp 57-67, Mar 1960;
[34] S. Schwartz and Y. S. Yeh "On the Distribution Function and Moments of Power Sums With Log Normal Components", Bell System Technical Journal, 1982;
[35] Radiocommunication Bureau, "DTTB Handbook – Digital terrestrial television broadcasting in the VHF/UHF bands", 2002;